RESEARCH REPORT R80-3

CRACK PROPAGATION MODES IN INJECTION MOLDED FIBER REINFORCED THERMOPLASTICS

by
J.F. Mandell
D.D. Huang
F.J. McGarry

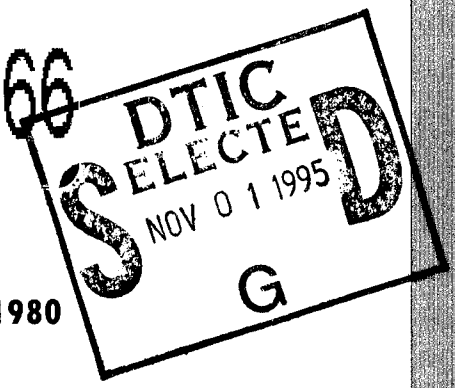

April 1980

MIT
DEPARTMENT
OF
MATERIALS SCIENCE
AND
ENGINEERING

SCHOOL OF ENGINEERING
MASSACHUSETTS INSTITUTE OF TECHNOLOGY
Cambridge, Massachusetts 02139

Sponsored by
The Lord Corporation

RESEARCH REPORT R80-3

CRACK PROPAGATION MODES IN INJECTION MOLDED FIBER REINFORCED THERMOPLASTICS

by

J.F. Mandell

D.D. Huang

F.J. McGarry

April 1980

Sponsored by

The Lord Corporation

School of Engineering

Massachusetts Institute of Technology

Cambridge, Massachusetts 02139

ABSTRACT

The modes of crack propagation are reported for injection molded short glass and carbon fiber reinforced thermoplastics. The matrices ranged from ductile to brittle, including Nylon 66, polycarbonate, polysulfone, poly(amide-imide), and polyphenylene sulfide; fiber contents were 30 or 40 % by weight. The main crack is found to grow in a fiber avoidance mode, bypassing regions of agglomeration of locally aligned fibers. The local mode of crack tip advance varied with matrix ductility and bond strength. The fracture toughness and fatigue resistance of each material are related to the mode of crack growth.

Introduction

The work described in this paper is closely related to recent papers on the fracture toughness [1] and fatigue resistance [2] of glass and carbon fiber reinforced injection molded thermoplastics. The materials used in these studies were reinforced with 30-40% by weight glass or carbon fibers; the matrices varied from ductile to very brittle. The fibers are oriented and broken down by the melt flow process, yielding a partially oriented system with variable fiber lengths. The distribution of fiber length, given in [2] for each material, showed a predominance of fragments with ℓ/d_f (length to diameter) ratios of less than twenty, and with the maximum fiber length less than one mm.

The fracture toughness in [1] was measured using notched tension specimens of various size. For a given direction and location on the reinforced specimens, a single-value fracture toughness, K_Q, appeared to be valid over most of the specimen size range [1]. Using the ultimate tensile strength (UTS) from ASTM D638 Type I bars, the crack-tip zone over which the UTS was exceeded, was calculated as

$$r_c \cong \frac{1}{2\pi} \left(\frac{K_Q}{UTS}\right)^2 \qquad (1)$$

Figure 1 shows that the calculated critical zone size correlates in magnitude and trend with the length of the longer fibers for each material, taken for convenience as the length exceeded by 5% of the fibers. The fracture specimens in this case had a crack length of 2.03 cm. The data suggest that for a given UTS, the fracture toughness is determined by the fiber length, regardless of fiber material, matrix ductility, or fiber/matrix bond strength. Table 1 lists the values of K_Q and UTS for each material; it should be noted that the K_Q values for the three tougher matrices - N66, PC, and PSUL, do not

appear to satisfy the plastic zone size requirement of the ASTM E399 test method, but these matrices are clearly very tough compared with PPS.

The S-N (maximum stress vs. log cycles to fail) fatigue behavior of these same materials was reported in [2]. Except for the N66 matrix systems, all S-N curves appeared linear over the entire loading range in tension-tension (R=.1) fatigue. The glass reinforced materials all lost between 10.5 and 11.4% of their strength per decade of cycles as shown in Table 1, close to the value observed for other glass reinforced materials such as SMC and unidirectional-ply laminates [3]. The carbon reinforced materials showed more variation in fatigue resistance, best for the brittle matrices, and worst for the ductile ones.

In each of the above studies, the mode of crack growth was observed to involve single macroscopic cracks which characteristically grow around the fibers on a local scale. The work described in this paper was intended to define the crack growth mechanisms for each material in an attempt to explain the fracture and fatigue behavior.

Experimental Methods

The matrix materials were all engineering thermoplastics including semicrystalline Nylon 66 (N66), amorphous polycarbonate (PC) and polysulfone (PSUL), as well as two higher temperature plastics, amorphous poly(amide-imide) (PAI) and semicrystalline polyphenylene sulfide (PPS). The unreinforced PPS is very brittle at room temperature, while the N66, PC, and PSUL all neck and draw in uniaxial tension. The PAI shows slight ductility in tension, but is most notable for a high elastic strain capability and high tensile strength. The fibers used were E-glass or PAN-based carbon with a modulus of approximately

207 GPa. The fiber surface treatments or coupling agents where present are proprietary formulations of the material suppliers given in [1,2]. The fiber content was 40% by weight, except 30% for the PAI systems; these are high values for this class of materials.

The specimens used in this study were end-gated ASTM D638 Type I tensile bars. The fiber orientation is variable, but the dominant direction is along the specimen length. Cracks were grown across the width, normal to the dominant fiber orientation. The loading was either tension-tension fatigue as described in [2], or wedge loading at a precut notch in a microscope loading fixture. Earlier fatigue work [2] was done using the same lot of specimens, while the fracture work [1] used larger plaques, but with the crack in the same direction relative to the fiber orientation. All tests were conducted in an air conditioned laboratory atmosphere.

Results and Discussion

Fiber Avoidance Mode of Crack Growth

Cracks in all of the reinforced materials propagated in such a manner as to avoid most of the fibers, as suggested in previous studies [1-3]. Figure 2 illustrates this mode in low magnification micrographs which, at this scale, are typical of all materials studied. The planar view gives the most detailed information about the crack path. The specimen in this case has been metallographically polished on the surface with sufficient care to avoid any damage such as fiber cracking. After the surface is prepared and inspected at high magnification, a crack is grown in the desired direction by forcing a wedge into a precut notch. The crack growth is generally stable, so that the crack tip can be observed at the desired magnification in a

light microscope as it propagates.

Figure 2 and subsequent micrographs indicate that the fibers tend to agglomerate into small groups with roughly parallel orientation. The length of these local agglomerations tends to be similar to the length of the longest fibers in the region. However, it should be noted that a planar surface seldom exposes the fiber over its entire length, and the fibers appear somewhat shorter in these micrographs than they actually are. They usually are either cut by the surface or plunge back into the interior after some exposed distance. Observation of all reinforced materials at low magnification as in Figure 2, reveals that the crack follows a path which avoids these agglomerated fiber groups as much as possible. This leaves a zig-zag appearance as shown. Interactions of the crack with more isolated fibers not associated with the agglomerations results in some debonded and pulled-out or broken fibers on the fracture surface. Studies of the fracture surface commonly conducted in the scanning electron microscope (SEM), fail to reveal information about the interactions of the crack with the fiber agglomerations which appear to dictate its path for this group of materials.

The SEM view at low magnification in Figure 2 does indicate that the planar zig-zag path on the surface is repeated in the thickness direction as well. Thus, a crack front will not define a flat plane, but will be moving locally in different directions at different positions through the thickness, depending upon the local fiber arrangement. The various parts of the crack front must finally join together to form a continuous zig-zag path by breaking away any material between the local growth regions. On a given plane such as that in Figure 2 (top), the local crack must frequently be redirected along the main crack path rather than continuing along a direction

more nearly parallel to the fibers to give a single macroscopic crack identity. On a given plane, the crack path is strongly influenced by the development of the crack on adjacent planes above and below that level. The implications of the fiber avoidance mode for the crack resistance of the material will be discussed later.

Local Mechanisms of Crack Advance

The fracture toughness may be predictable simply from the gross nature of the fiber avoidance mode, as will be discussed later. However, the fatigue resistance appears to be sensitive to the local mechanisms of crack advance. This section will present observations of the mechanisms involved for each material as viewed during static loading in the microscope and after fatigue loading in a servo-hydraulic machine. It is difficult to obtain clear micrographs of what is readily observed in practice, and then only a sampling of hundreds of micrographs can be presented here due to length limitations. While most of the micrographs presented are planar surface views of static cracks grown in a stepwise fashion by loading increments, an attempt is made to relate these results to observations of the crack on the interior of the specimen and to fatigue cracks.

Figures 3 and 4 show the local mode of crack growth for the very brittle PPS matrix with glass and carbon fibers. The details of each are surprisingly different. The development of the crack tip zone is shown for the glass system in Figure 3 at four successively higher loads. The crack path can be correlated from one micrograph to the next by the arrow locations. There is a region ahead of the main crack in which small separate cracks are formed, mostly around fiber ends. These cracks coalesce at higher loads to form the main crack. This mode results in cracks primarily in the matrix and across fiber

ends, with little fiber pullout. Occasional fibers are broken by the crack, such as the one indicated by the lower arrow in (d). The PPS systems tend to contain many voids, which appear as dark circles in Figure 3.

The same matrix with carbon fibers in Figure 4 shows much more tendency to debond and pull out fibers. Little or no local cracking around the main crack tip (c) is observed. The crack in the matrix appears to grow past debonded fibers, and then extract them from the matrix as it opens. However, the crack still grows around the major agglomerations of fibers as described earlier. Many of the debonded fibers appear to slide uniformly out of the matrix as shown by the lower arrow in (a). Such sliding requires that the main crack open along the fiber axis, since the fiber is rigid and does not distort significantly. The upper arrow in (a) indicates a fiber at another angle. This fiber is oriented in a different direction, and cannot slide out of its matrix sheath with the main crack opening in the direction dictated by the fibers on either side and possibly other fibers in the interior. Being on the surface, this fiber could pull free to accommodate the situation, but some such fibers are observed to break if they are bent across a crack which opens in a direction other than along the individual fiber axis. Such local variations in fiber orientation may contribute significantly to crack resistance, requiring fiber failure or matrix fragmentation before the main crack can open, even with the relatively small deviation in fiber alignment shown in Figure 4(a). It appears that a major difference between the glass and carbon systems may be a much lower bond strength in the carbon system, but direct bond strength measurements have not been made.

Figure 5 shows a distinctly different local mode of extension for

the carbon reinforced polycarbonate, which is typical of most of the ductile matrix systems. The main crack tip shown in (d) is actually a local continuous band of yielding and necking, with some fiber pull-out. Further back along the main crack (c) the yielded material tears apart in some regions, and finally the whole yielded path tears apart to form a real crack. The arrows (lower right) in (a) and (b) show the same spot before and after crack growth. The region ahead of the crack contains many locally yielded areas, especially near fiber ends, such as at the arrow. These coalesce to form the main continuous yielded zone, which later tears apart to form the crack. As in the PPS/glass, this coalescence mode allows the crack to seek out the path of least resistance, with occasional fibers crossed by the main yield zone extracted from the matrix. Figure 6 shows the same features for carbon reinforced polysulfone and Nylon 66.

The ductile matrices with glass fibers show a similar mode of local ductile crack growth, as in Figure 7(b) for the Nylon 66 matrix. A combined mode is evident for the glass reinforced polycarbonate in Figure 7(a). Widespread local cracks or crazes are formed ahead of the main crack, mostly near fiber ends. However, close to the main crack tip local necking and yielding appears to dominate. In each of the glass reinforced systems, fibers were occasionally observed to break where they bridged the main crack or yield band; fiber failure was rarely observed with carbon fibers.

The poly(amide-imide) matrix does not neck and draw in uniaxial tension, but shows considerable local ductility in the composite. Figure 8 shows a crack tip and subsequent growth for the carbon reinforced system. The carbon fibers in this material are kidney-shaped in cross-section, giving a split appearance when polished part-way through. Local tearing of the yielded material is evident to the left

of the arrow in (b). Figure 9 shows the development of damage at a notch root in the glass reinforced system. The arrows in (a) and (b) trace the development of fiber debonding (which occurred first), yielding, and fiber fracture. (The fiber at the immediate notch boundary was cracked during notching.) The crack path (c) shows a broken fiber (arrows), and debonded, pulled-out fibers. Yielding was very localized in the PAI systems, but the brittle cracking observed in glass/PPS around fiber ends was not evident. Instead, the high strain capacity of the matrix appeared to result in fiber debonding and fracture, along with some local yielding.

Differences in the local mode of crack growth are also observed in SEM micrographs of the fracture surfaces. The carbon reinforced systems in Figure 10 show variations from brittle matrix fracture for PPS to very ductile for N66, with some ductility evident for PC and PAI. The same sequence with glass fibers in Figure 11 (lower magnification than Fig. 10) shows similar effects. However, relatively few fibers are observed on the PPS surface, reflecting the local mode of formation of the crack in Figure 3.

Figures 12-14 are an attempt to define the local crack growth modes observed using schematics with an arbitrary fiber arrangement. Figure 12 represents the local cracking, crack coalescence mode of PPS/glass, with occasional fiber failure. Figure 13 represents the PPS/carbon system with poor bonding, showing frequent fiber debonding and pullout. Figure 14 represents the ductile matrix systems, with local yielding ahead of the crack followed by coalescence into a main yielded zone which eventually tears to form a crack. Here, the dark areas at the fiber ends represent yielding, while the light gaps represent separation.

It is important to note that these results are primarily from examination of cracks on the surface. Polishing of the material after crack growth to observe the interior tends to smear the matrix detail. However, such observation coupled with the observation of cross-sections of crack-tips indicates that the surface results generally also apply to the interior. The brittle matrix growth mechanisms are unchanged. The ductile systems cannot form a continuous local necked zone, but form voids between drawn regions. The ductility in the interior is also evident in the SEM micrographs. Much of the ductility appears to be in response to shear stresses resulting from relative movement of adjacent groups of fibers, rather than plane-stress effects at the surface. SEM investigation revealed no significant increase in drawn, yielded material at the surface, as might be expected of plane stress effects.

The effect of fatigue cycling on the mode of crack growth was determined by growing fatigue cracks across previously polished specimens of each material, then observing under slight load in the microscope. Although damage such as local cracking near fiber ends may have been slightly more widespread in fatigue, no significant differences from static cracks in the mode of growth or the fracture surface could be identified. Some isolated regions of fatigue striations on cracks around fiber ends were reported in [2], but it was generally not possible to distinguish a fatigue crack from a static crack.

Interpretation of Fracture and Fatigue Data

Fracture Toughness. The micrographs clearly give several possible alternatives for explaining the fracture toughness. The traditional approach would concentrate on the fiber pullout friction and debonding energy [4], as well as ductile flow where present. However,

the empirical findings represented in Figure 1 suggest a criterion which does not depend directly on the local mechanisms of crack resistance. All of the data in Figure 1 were for cracks greater than 2 cm. in length, at least 40 times the long fiber length or calculated crack tip zone radius. Thus, all of the long fibers and agglomerations should be embedded in the singular crack tip stress field, and the calculation of K_I at fracture should be valid [5].

The fracture criterion which has been suggested for the fiber avoidance mode [1] postulates that the crack should be able to propagate if the local stress reaches the UTS at a critical distance, r_c, from the crack tip similar to the length of the longer fibers in the distribution, termed ℓ_f^* (taken in Figure 2 for convenience as the length exceeded by 5% of the fibers). For the fiber arrangement assumed in the schematics, this distance would be represented as in Figure 15. Since this condition is reached all through the thickness, the zig-zag crack front evidenced in Figure 2 should be able to grow around any long fiber or agglomeration and move in a macroscopic sense.

Calculation of the critical crack tip dimension mixes microstructure with continuum mechanics, and is clearly very approximate in nature. Ignoring directional effects, the local stresses around the crack tip are approximately [5]

$$\text{local stresses} \cong \frac{K_I}{(2\pi r)^{1/2}} \qquad (2)$$

Where r is the distance form the crack tip. The crack will propagate by this criterion when the local stress reaches the UTS at a critical radius r_c equal to the length of the longer fibers or agglomerations,

$$r_c = \ell_f^* \cong \frac{1}{2\pi} \left(\frac{K_I}{UTS}\right)^2 \quad (3)$$

and at this condition K_I will be the fracture toughness, K_Q, so that

$$K_Q \cong UTS(2\pi \ell_f^*)^{1/2} \quad (4)$$

This relationship appears to be in agreement with the data in Figure 1. The great variation in matrix toughness and apparent bond strength evident for this group of materials seems not to greatly influence the fracture toughness. What influence the constituent and interface properties do have enters through the UTS, and even that is modest (Table 1). The UTS is also likely to depend on fiber length for these materials [4].

Fatigue Effects. Fatigue appears to involve the gradual development and extension of cracks in all of these materials [2]. While the fracture toughness does not appear to be influenced by the local details of crack advance, cycling the material at less than the critical load may give more sensitivity. The similar rate of degradation in fatigue of the glass reinforced systems to that observed for chopped strand and continuous fiber glass/ epoxy discussed earlier [2,3], indicates that fatigue may be a fiber-sensitive property for glass reinforced materials. The observation of occasional glass fiber failure in each material supports this view. By implication, the few fibers which are not avoided or pulled out by the crack, but finally must be broken, may determine the fatigue resistance.

Carbon fiber composites generally show very little degradation in fatigue for long fiber unidirectional materials [6]. Carbon fiber failures were very rarely observed in this study in fatigue or static

crack growth. These observations appear to leave only the matrix and interface to influence the fatigue of the carbon reinforced materials, and a significant sensitivity to the matrix material was observed in [2] (Table 1). The best fatigue resistance is provided by the brittle PPS matrix system which tends to have many debonded fibers bridging the crack. Their effect is to provide force transfer across the crack faces by friction or by the interlocking mechanism of fibers with different orientation described earlier. A tensile test of a specimen cut from a fatigue crack tip was reported in [2] to support a stress of 24 MPa. Fatigue of the ductile matrix materials appears to involve cyclic failure of the yielded matrix ahead of the crack tip, and poorer fatigue resistance is obtained.

Discussion

The conventional view of the strength and crack resistance of short fiber composites has been closely tied to the concepts of the critical fiber length, ℓ_c [4]. The critical length is that which is sufficient to allow the stress transferred through shear at the interface to load the fiber to failure. This model involves an isolated fiber oriented parallel to the applied uniaxial tensile stress. The impact and crack resistance are often viewed as deriving from the work of extracting fibers or pieces of fibers shorter than ℓ_c from the crack surfaces [4,7]. It is difficult to envision the usefulness of the ℓ_c model for the relatively high fiber content, poorly aligned fiber cases studied here, due to the following observations:

1. Of the fibers which break, most appear to be bent across the crack, which does not open along their axis.

2. Cases in which the crack avoids nearly all of the fibers, such as PPS/glass, have strength and fracture toughness comparable to the other materials.
3. Since the fibers are not parallel aligned, they cannot all slide smoothly out of the matrix as the crack opens in one general direction. The fibers appear too stiff to bend appreciably as may occur in metal wire reinforced concrete [8].
4. The stresses applied to the fiber are complicated greatly by the cracking at the fiber ends, partial debonding, contact with adjacent fibers, etc.

The results suggest several points of interest in materials development. First, longer fibers are better for toughness as well as strength as long as the same modes of crack extension occur. It is doubtful that this observation would hold for significantly longer fibers, since they would be more likely to break. For fatigue resistance, little change appears likely for glass reinforced materials which lose approximately 10% of their UTS per decade of cycles under these loading conditions. For graphite reinforced materials, a brittle matrix, poorly bonded system seems to give the best fatigue performance, but with some loss in UTS, compared with a ductile or well bonded material.

Throughout this work the crack was grown normal to the dominant fiber orientation. Crack growth more nearly parallel to the fibers gives much lower values of K_Q for both brittle and ductile systems [1], but the observations presented here have not been examined in detail for this case. The relatively high fiber content used in this study may also have had a significant effect on the results. Micrographs

as shown in [7] suggest that the matrix crack may grow on a flatter plane rather than in a fiber-avoidance mode if the fiber content is significantly lower; if so, this could change all of the observations made in this study. Higher rate loading or lower temperatures will likely cause changes in the ductile systems. A mode change to brittle matrix behavior after some slow, ductile growth has been observed in very recent tests with the carbon reinforced Nylon 66 at a lower fiber content under the same loading conditions used in this study. At high rates this mode change has also been observed at 40% fiber content.

Conclusions

The main crack in each material appeared to follow a fiber avoidance mode, growing around the longer fibers and agglomerations of locally aligned fibers. A fracture criterion based on reaching the UTS at a distance from the crack tip equal to the length of the longer fibers is in agreement with fracture toughness data. The fatigue resistance appears to be more influenced by the local details of crack tip advance. Occasional fiber failure appears to dominate the fatigue resistance of glass fiber systems, resulting in behavior similar to other glass reinforced plastics. The matrix and interface are more important for the graphite reinforced materials, where a brittle matrix, poorly bonded system gave the best performance and a distinctive mode of crack advance.

Acknowledgements

This work was sponsored by the Lord Corporation, and materials were molded and supplied by its Keyon Materials facility. The work of George Normann in specimen preparation is also appreciated.

References

1. Mandell, J.F., Darwish, A.Y., and McGarry, F.J., "Fracture Testing of Injection Molded Glass and Carbon Fiber Reinforced Thermoplastics," presented at ASTM Symp. "Test Methods and Design Allowables for Fibrous Composites," Dearborn, MI (1979).

2. Mandell, J.F., Huang, D.D. and McGarry, F.J., "Fatigue of Glass and Carbon Fiber Reinforced Engineering Thermoplastics," Proc. 35th RP/C Institute, Society of the Plastics Industry, New Orleans (1980) paper 20-D.

3. Mandell, J.F., "Fatigue Crack Growth in Fiber Reinforced Composites," Proc. 34th RP/C Institute, Society of the Plastics Industry, New Orleans (1979) paper 20-C.

4. Kelly, A., Strong Solids, 2nd. ed., Clarendon Press, Oxford (1973) p.157.

5. Knott, J.F., Fundamentals of Fracture Mechanics, Butterworths, Boston (1973) p. 133.

6. Dharan, C.K.H.,"Fatigue Failure Mechanisms in Pultruded Graphite -Polyester Composites," in Failure Modes in Composites II, J.N. Fleck and R.L. Mehan, eds., The Metallurgical Society of AIME, New York (1974) p. 144.

7. Ramsteiner, F. and Theysohn, R., "Tensile and Impact Strengths of Unidirectional, Short-Fiber-Reinforced Thermoplastics," Composites, Vo. 10 (1979) p. 111.

8. Naaman, A. E., Argon, A.S., and Moavenzadeh, F., "A Fracture Model for Fiber Reinforced Cementitious Materials," Cement and Concrete Research, vol. 3 (1973) p. 397.

Table 1. Strength, Fracture Toughness and Fatigue Properties [1,2].

Property	Reinforcement	Matrix				
		N66	PC	PSUL	PPS	PAI
K_Q	none*	10.9	8.4	4.7	0.8	---
($MNm^{-3/2}$)	glass	9.9	8.7	6.5	7.0	9.4
	carbon	9.4	7.5	7.2	6.6	---
UTS	none**	74	72	77	35	140
(MPa)	glass	181	161	158***	181	203
	carbon	256	203	197	156	231
% Loss of UTS/Decade Fatigue Cycles	glass	10.9	11.4	---	10.9	10.5
	carbon	9.9	11.5	11.1	7.8	9.5

* K_Q data for N66 and PC do not satisfy validity criteria of ASTM E399.

** Values for N66, PC, PSUL are yield stress

*** Estimated value [1].

Figure Captions

Figure	Caption
1	Calculated Critical Zone Radius vs. Fiber Length Exceeded by 5% of Fibers; Various Carbon and Glass Fiber Reinforced Thermoplastics with 30 to 40% Fiber by Weight [1].
2	Low Magnification Views of Fiber Avoidance Mode of Crack Growth in Carbon Fiber Reinforced Polycarbonate (Top, Planar View in Light Microscope); and Nylon 66 (Bottom, SEM Fractograph); ($d_f \cong 10\mu m$).
3	Crack Tip in Glass Reinforced Polyphenylene Sulfide Under Increasing Load (a) - (d); Arrows Indicate Path Crack Will Follow; ($d_f \cong 11\mu m$).
4	Various Positions Along Crack in Carbon Reinforced Polyphenylene Sulfide; ($d_f \cong 10\mu m$).
5	Crack in PC/C; (c) and (d) are Magnified Views of Crack in Position (a); (b) is Same Area as (a), but After Crack Growth; Crack Path Indicated by Arrows in (a) and (b); ($d_f \cong 10\mu m$).
6	Cracks in Carbon Reinforced Polysulfone (a); and Nylon 66 (b) Along Crack, and (c) at Tip; ($d_f \cong 10\mu m$).
7	Crack Tip in Glass Reinforced Polycarbonate (a), and Nylon 66 (b); ($d_f \cong 11\mu m$).

Figure Captions
(continued)

Figure	Caption
8	Crack Tip (a) in Carbon Reinforced Poly(Amide-Imide), and Same Region After Crack Extension (b); Arrows Indicate Crack Path; ($d_f \cong 15\mu m$)
9	Glass Reinforced Poly(Amide-Imide) Showing Damage Development at Notch Root at Low (a) and High (b) Loads, and Crack Path (c); ($d_f \cong 11\mu m$).
10	Fracture Surfaces of Carbon Reinforced Matrices; Clockwise from Upper Left: Polyphenylene Sulfide, Poly(Amide-Imide), Nylon 66, Polycarbonate; ($d_f \cong 10\mu m$).
11	Fracture Surfaces of Glass Reinforced Matrices; Clockwise From Upper Left: Polyphenylene Sulfide, Poly(Amide-Imide), Nylon 66, Polycarbonate; ($d_f \cong 11\mu m$).
12	Schematic of Local Mode of Crack Growth in Well-Bonded, Brittle Matrix, Glass Fiber Material.
13	Schematic of Local Mode of Crack Growth in Poorly Bonded, Brittle Matrix Material.
14	Schematic of Local Mode of Crack Growth in Ductile Matrix Material.
15	Model for Critical Crack Tip Zone Radius for Fiber-Avoidance Mode of Fracture.

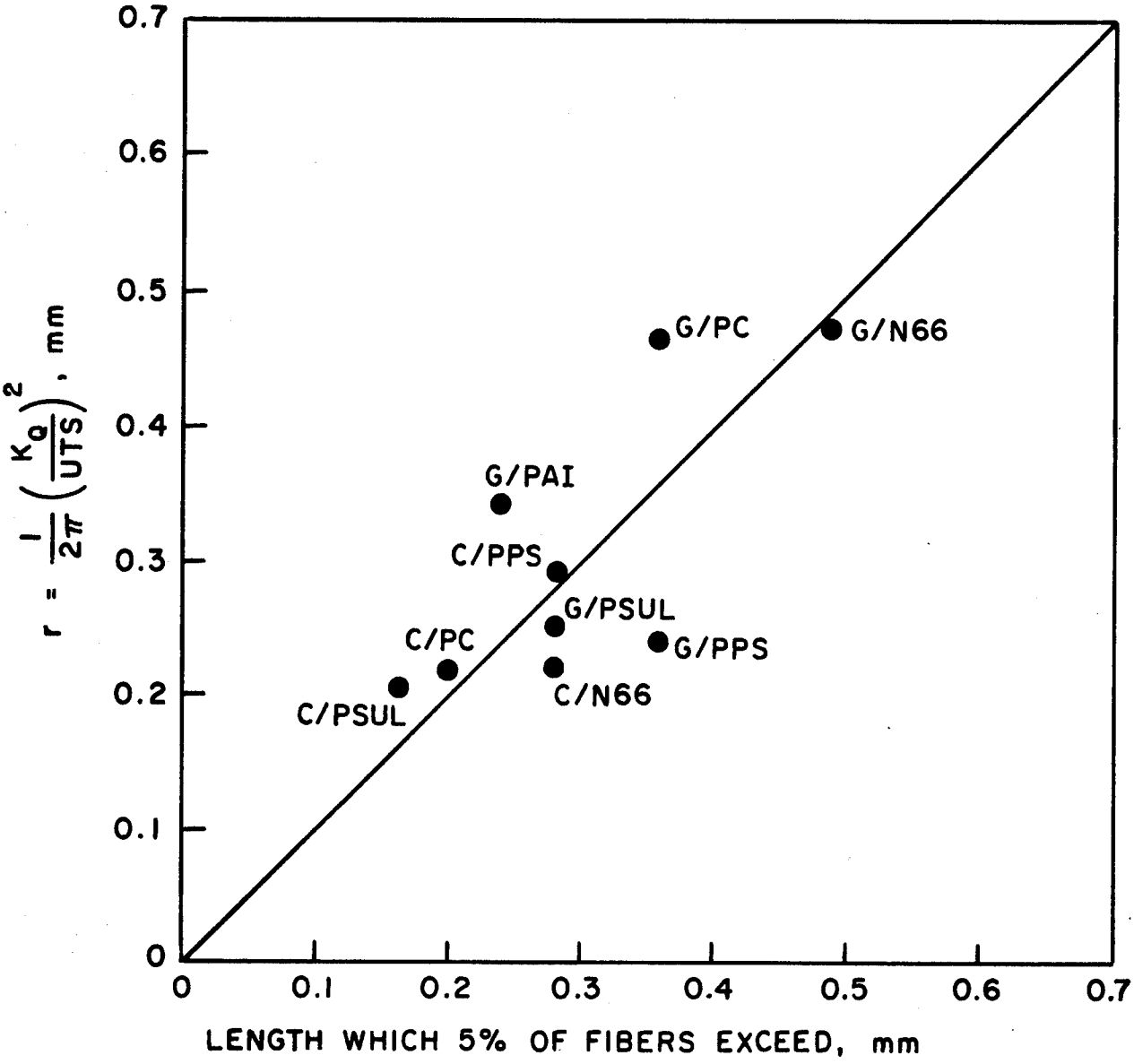

FIGURE 1

CALCULATED PLASTIC ZONE RADIUS vs. FIBER LENGTH EXCEEDED BY 5% OF FIBERS; VARIOUS CARBON AND GLASS FIBER REINFORCED THERMOPLASTICS WITH 30 TO 40% FIBER BY WEIGHT [1].

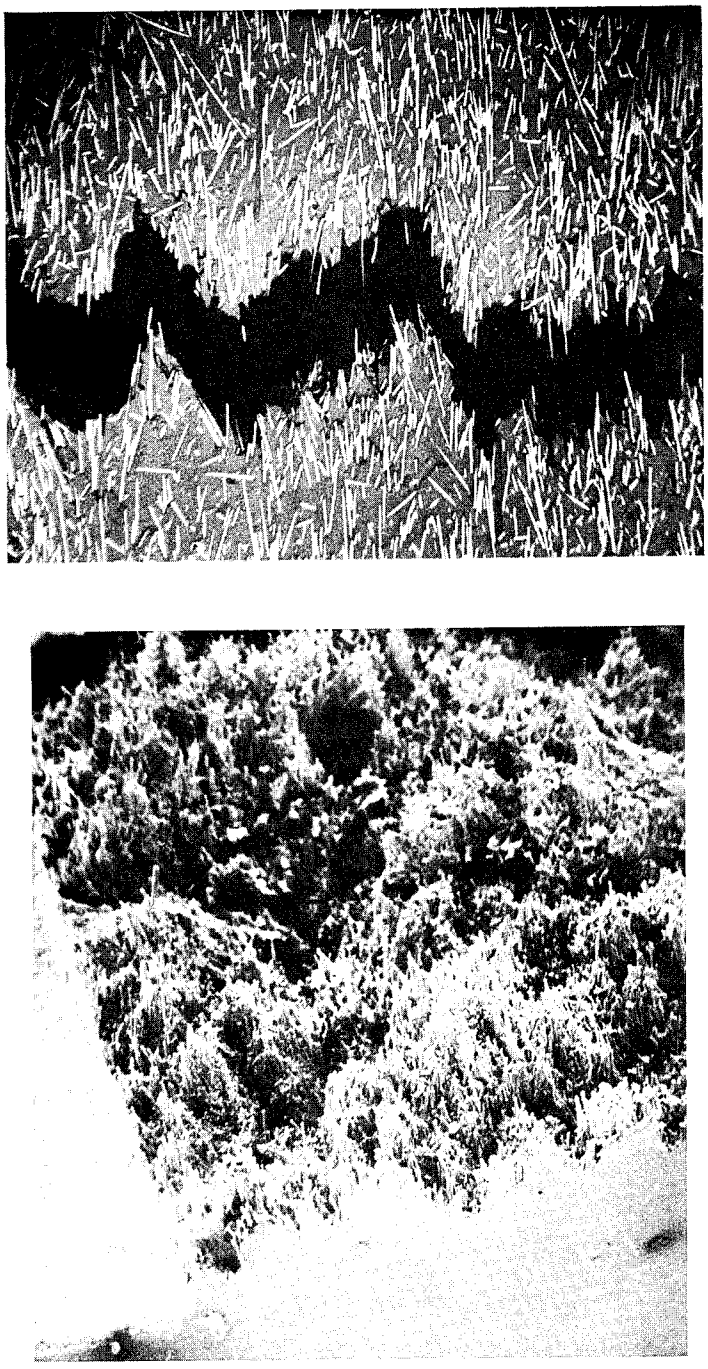

FIGURE 2.

LOW MAGNIFICATION VIEWS OF FIBER AVOIDANCE MODE OF CRACK GROWTH IN CARBON FIBER REINFORCED POLYCARBONATE (TOP, PLANAR VIEW IN LIGHT MICROSCOPE); AND NYLON 66 (BOTTOM, SEM FRACTOGRAPH); ($d_f \cong 10\,\mu m$).

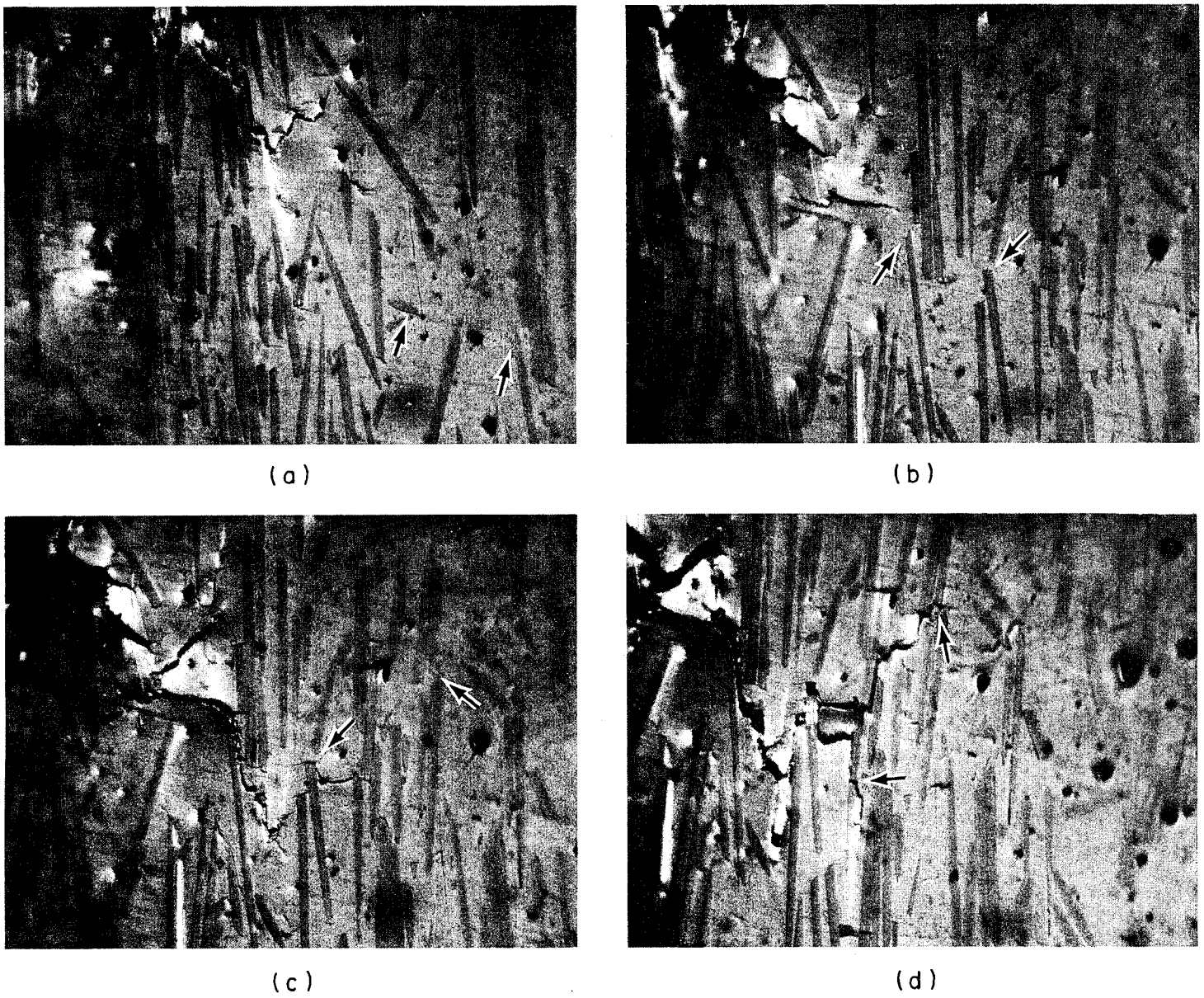

FIGURE 3.

CRACK TIP IN POLYPHENYLENE SULFIDE UNDER INCREASING LOAD (a) - (d); ARROWS INDICATE PATH CRACK WILL FOLLOW; ($d_f \cong 11\,\mu$ m).

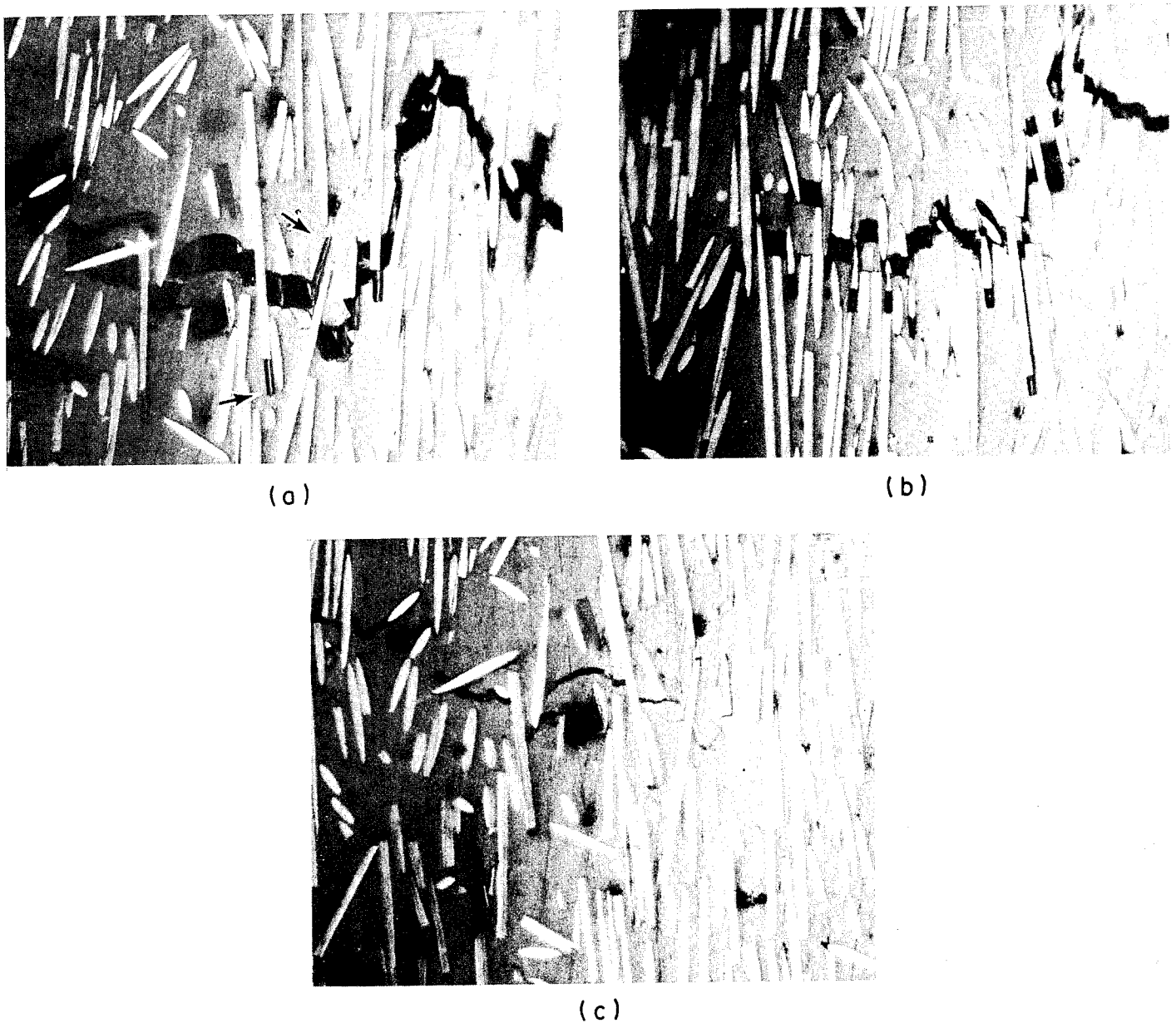

FIGURE 4.

VARIOUS POSITIONS ALONG CRACK IN CARBON REINFORCED POLYPHENYLENE SULFIDE; ($d_f \cong 10\,\mu m$).

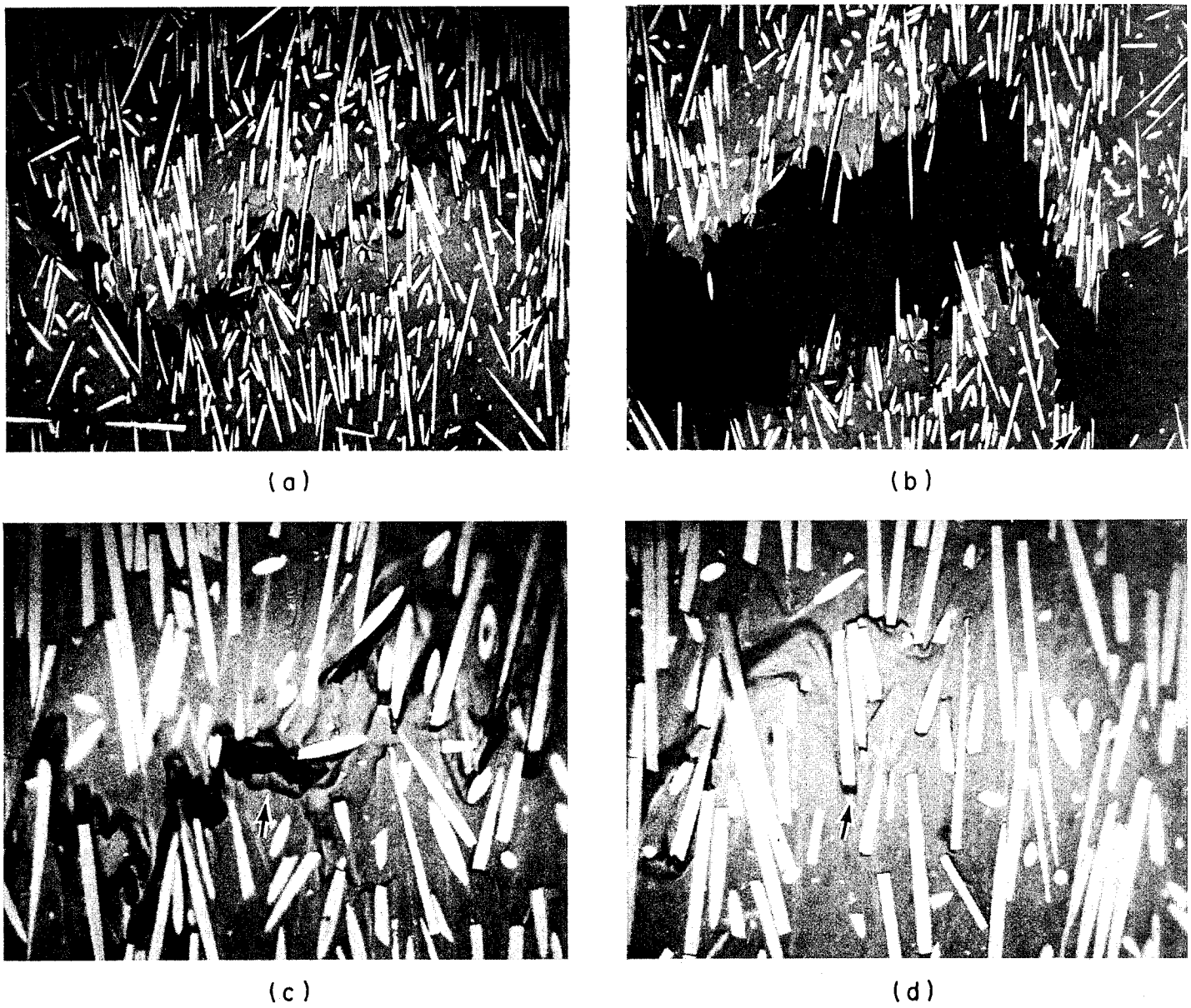

FIGURE 5.

CRACK IN PC/C; (c) AND (d) ARE MAGNIFIED VIEWS OF CRACK IN POSITION (a); (b) IS SAME AREA AS (a), BUT AFTER CRACK GROWTH; CRACK PATH INDICATED BY ARROWS IN (a) AND (b); ($d_f \cong 10\ \mu m$).

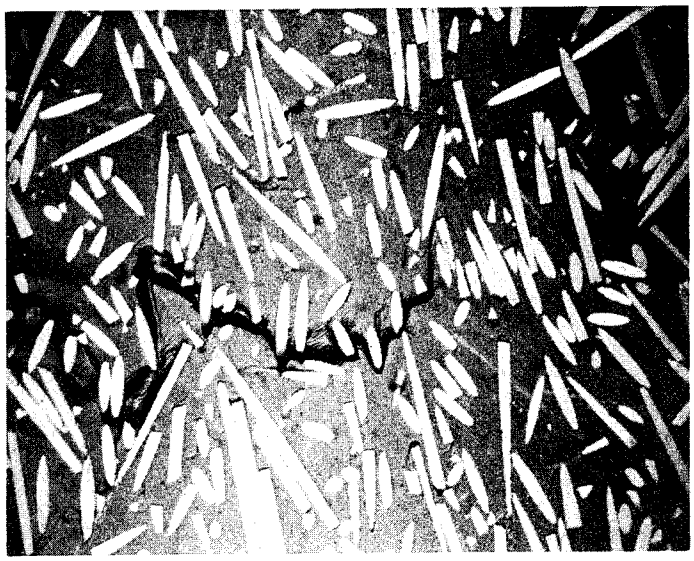

(a)

(b)

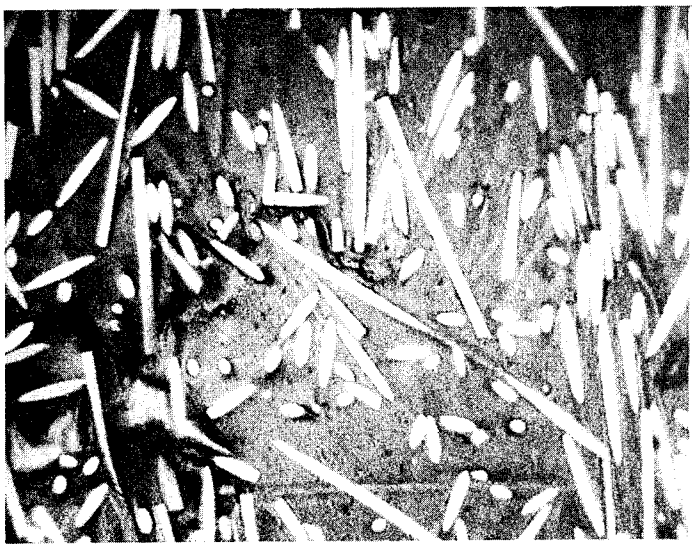

(c)

FIGURE 6.

CRACKS IN CARBON REINFORCED POLYSULFONE (a); AND NYLON 66 (b) ALONG CRACK, AND (c) AT TIP; ($d_f \cong 10\ \mu m$).

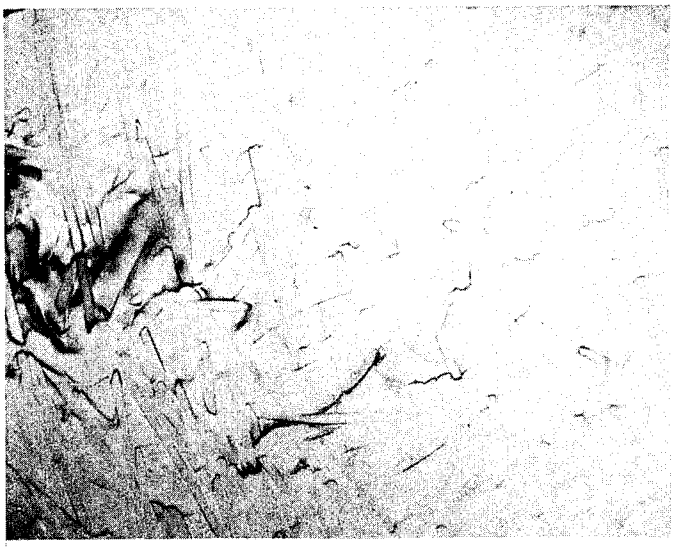

(a)

(b)

FIGURE 7 .

CRACK TIP IN GLASS REINFORCED POLYCARBONATE (a), AND NYLON 66 (b); ($d_f \cong 11\ \mu m$).

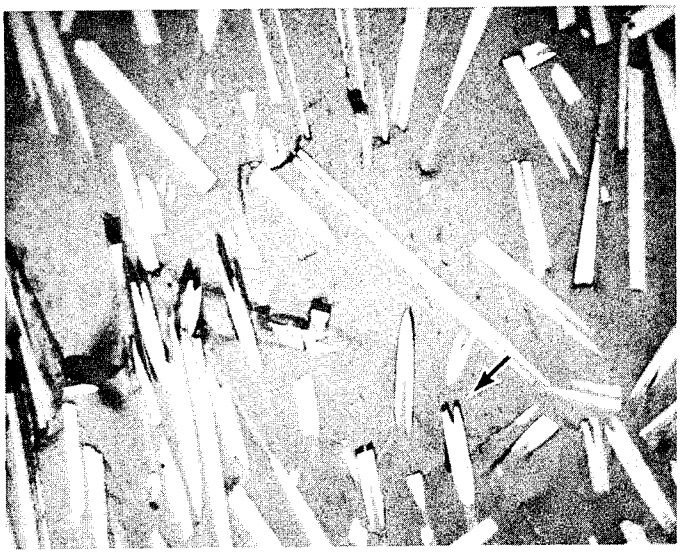

(a)

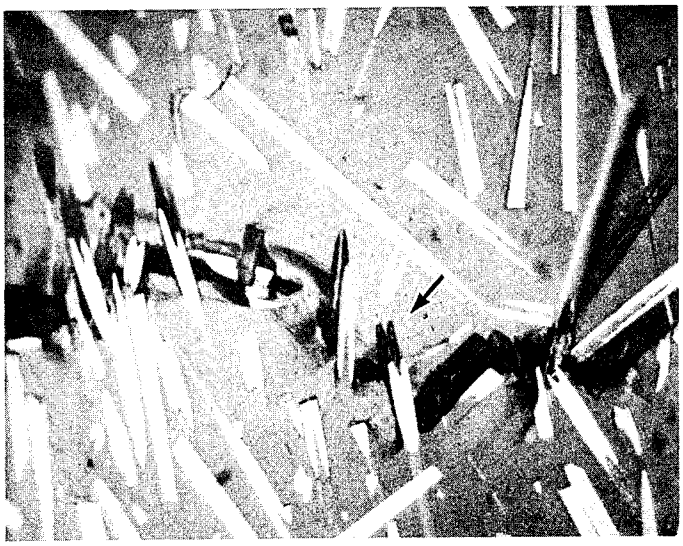

(b)

FIGURE 8 .

CRACK TIP (a) IN CARBON REINFORCED POLY(AMIDE-IMIDE), AND SAME REGION AFTER CRACK EXTENSION (b); ARROWS INDICATE CRACK PATH; ($d_f \cong 15\,\mu m$).

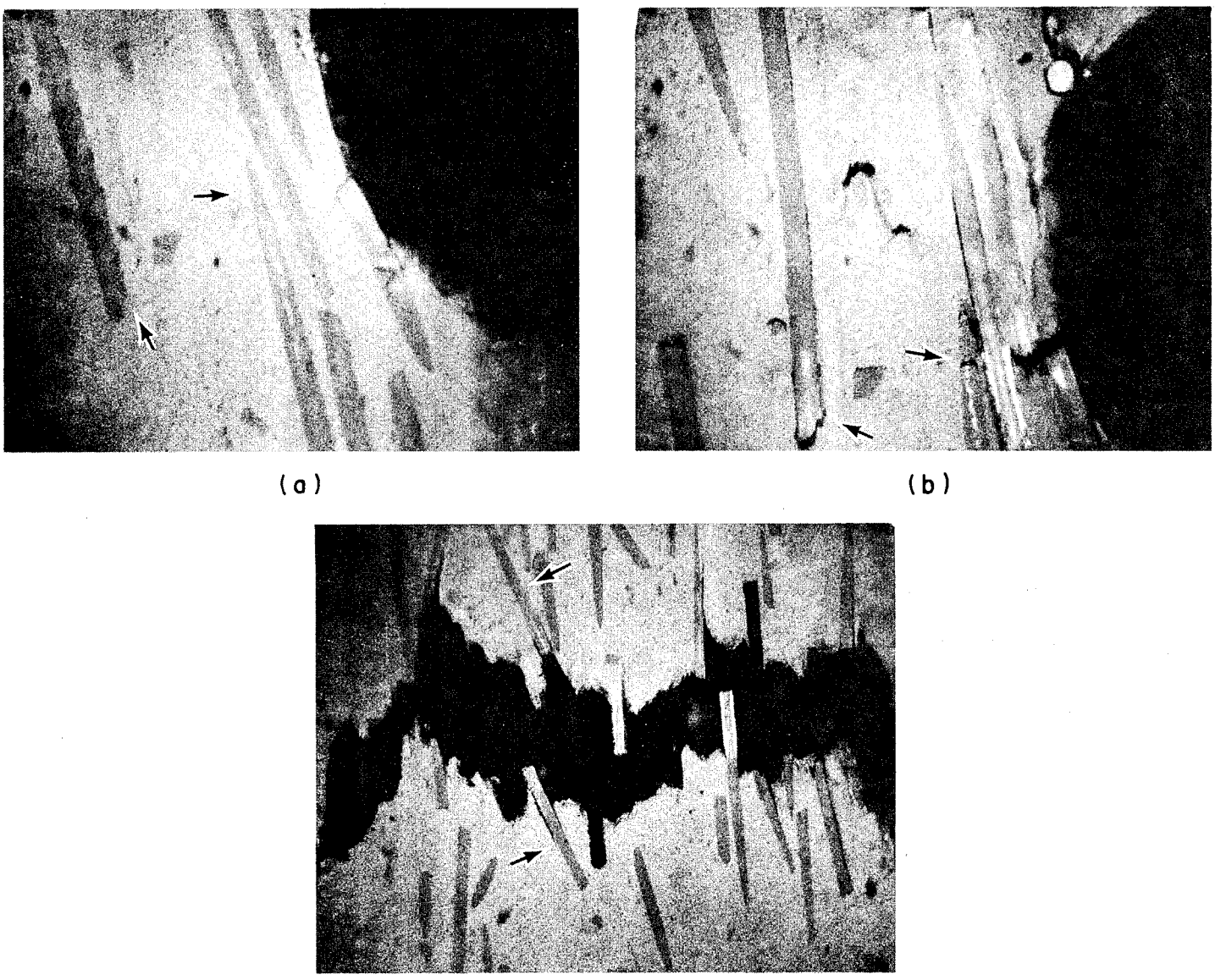

FIGURE 9.

GLASS REINFORCED POLY(AMIDE-IMIDE) SHOWING DAMAGE DEVELOPMENT AT NOTCH ROOT AT LOW (a) AND HIGH (b) LOADS, AND CRACK PATH (c); ($d_f \cong 11\,\mu$ m).

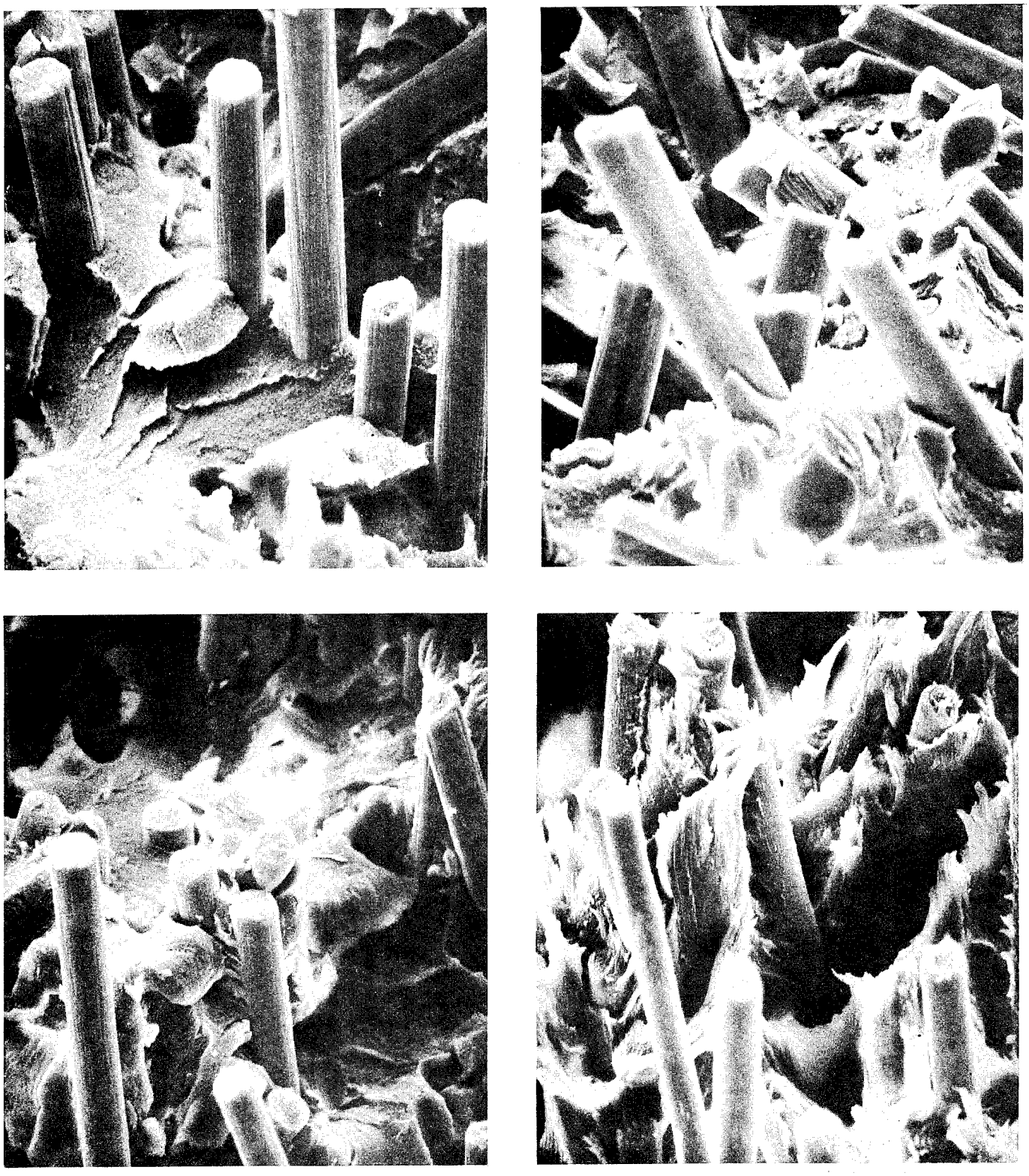

FIGURE 10.

FRACTURE SURFACES OF CARBON REINFORCED MATRICES; CLOCKWISE FROM UPPER LEFT: POLYPHENYLENE SULFIDE, POLY(AMIDE-IMIDE), NYLON 66, POLYCARBONATE; ($d_f \cong 10\,\mu m$).

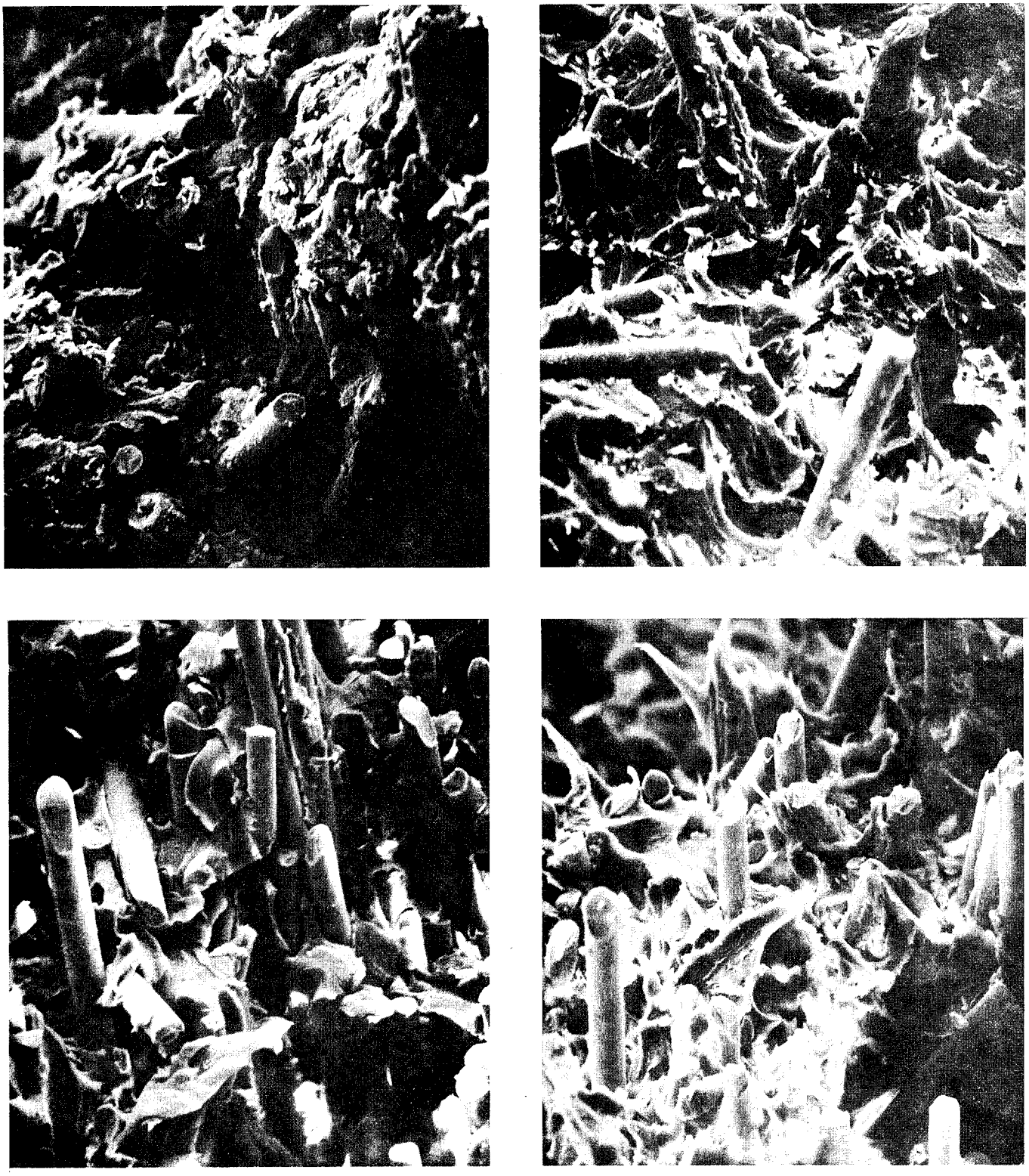

FIGURE 11.

FRACTURE SURFACES OF GLASS REINFORCED MATRICES; CLOCKWISE FROM UPPER LEFT: POLYPHENYLENE SULFIDE, POLY(AMIDE-IMIDE), NYLON 66, POLYCARBONATE; ($d_f \cong 11\ \mu m$).

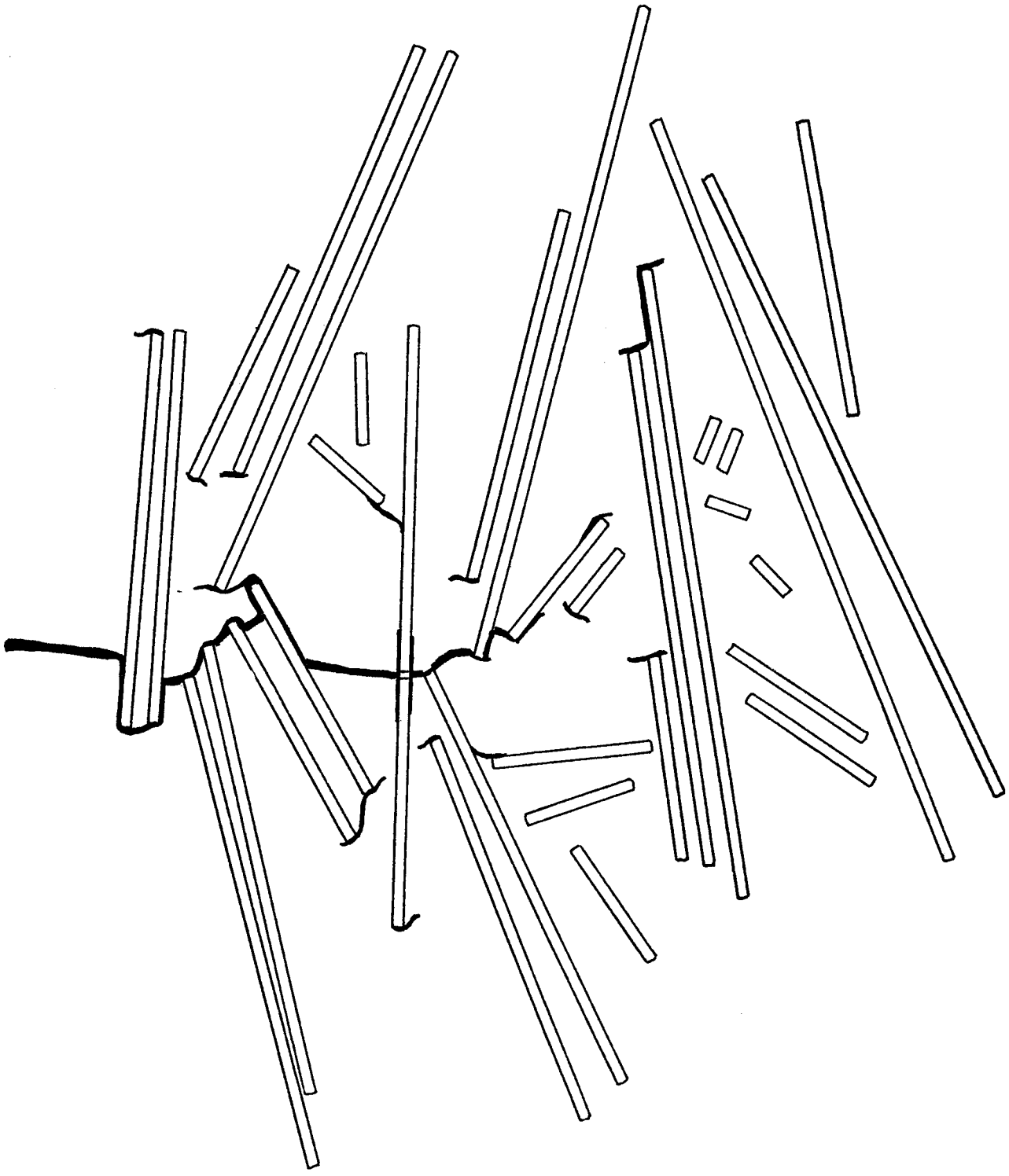

FIGURE 12.

SCHEMATIC OF LOCAL MODE OF CRACK GROWTH IN WELL-BONDED, BRITTLE MATRIX, GLASS FIBER MATERIAL.

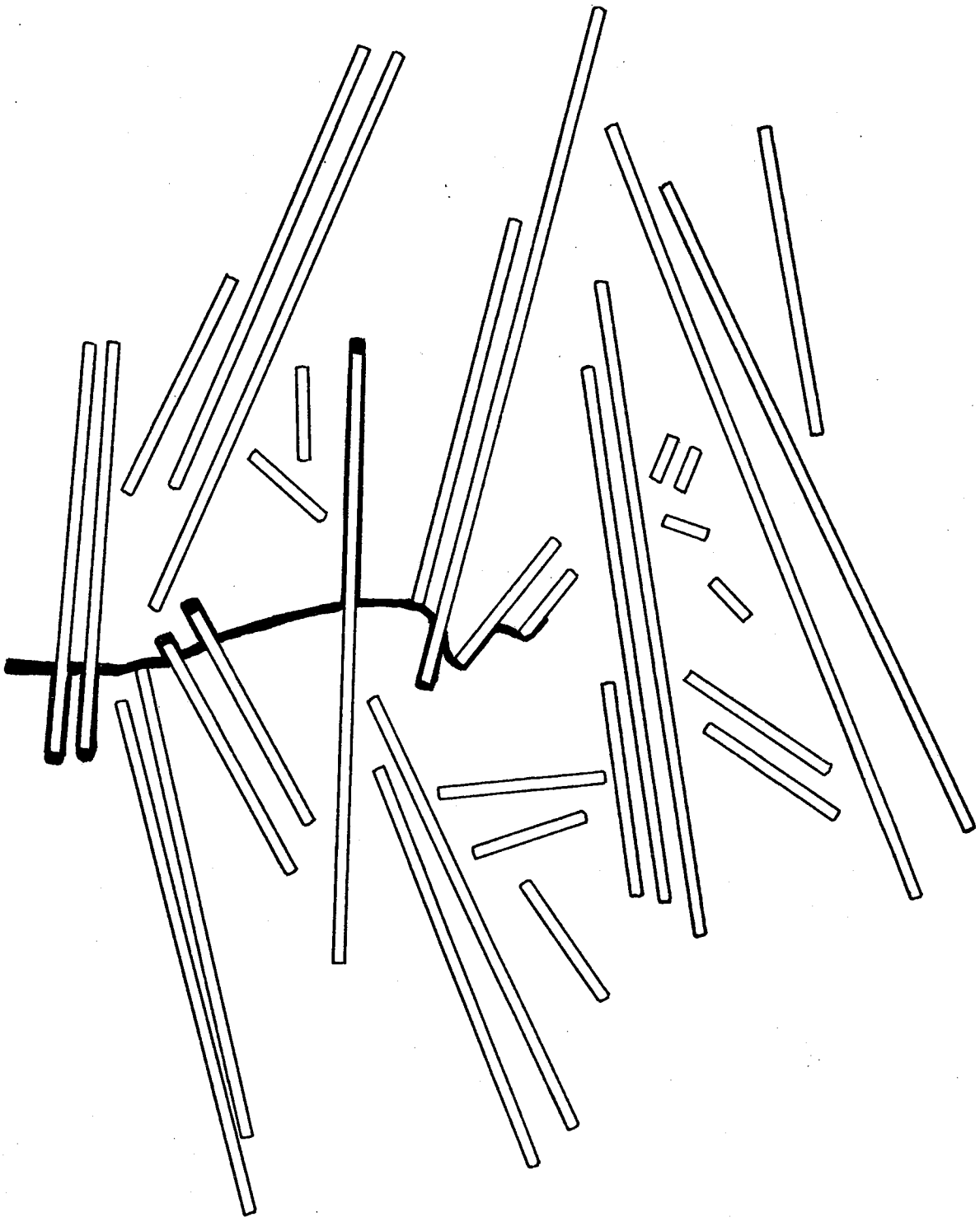

FIGURE 13.

SCHEMATIC OF LOCAL MODE OF CRACK GROWTH IN POORLY BONDED, BRITTLE MATRIX MATERIAL.

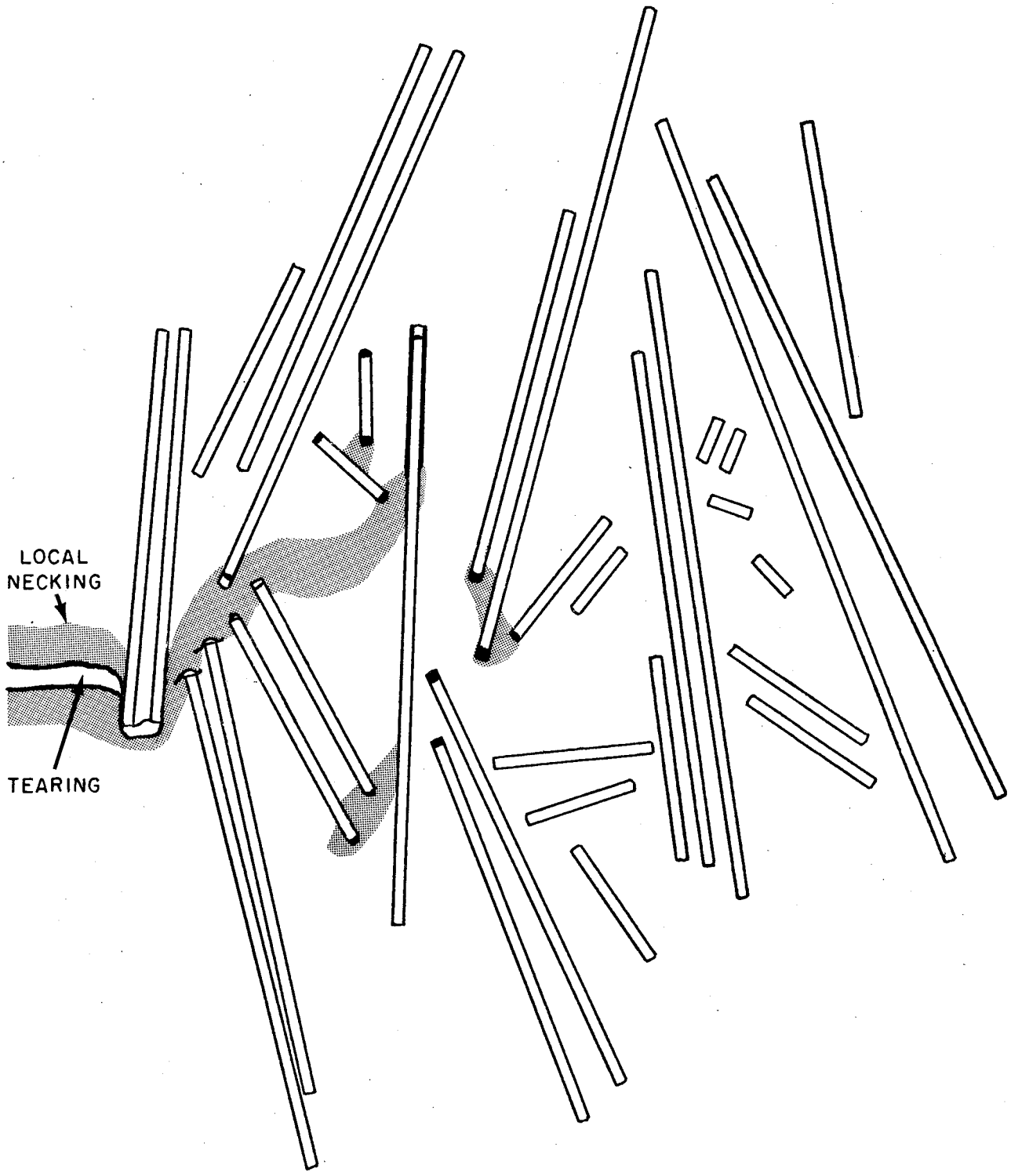

FIGURE 14.

SCHEMATIC OF LOCAL MODE OF CRACK GROWTH IN DUCTILE MATRIX MATERIAL.

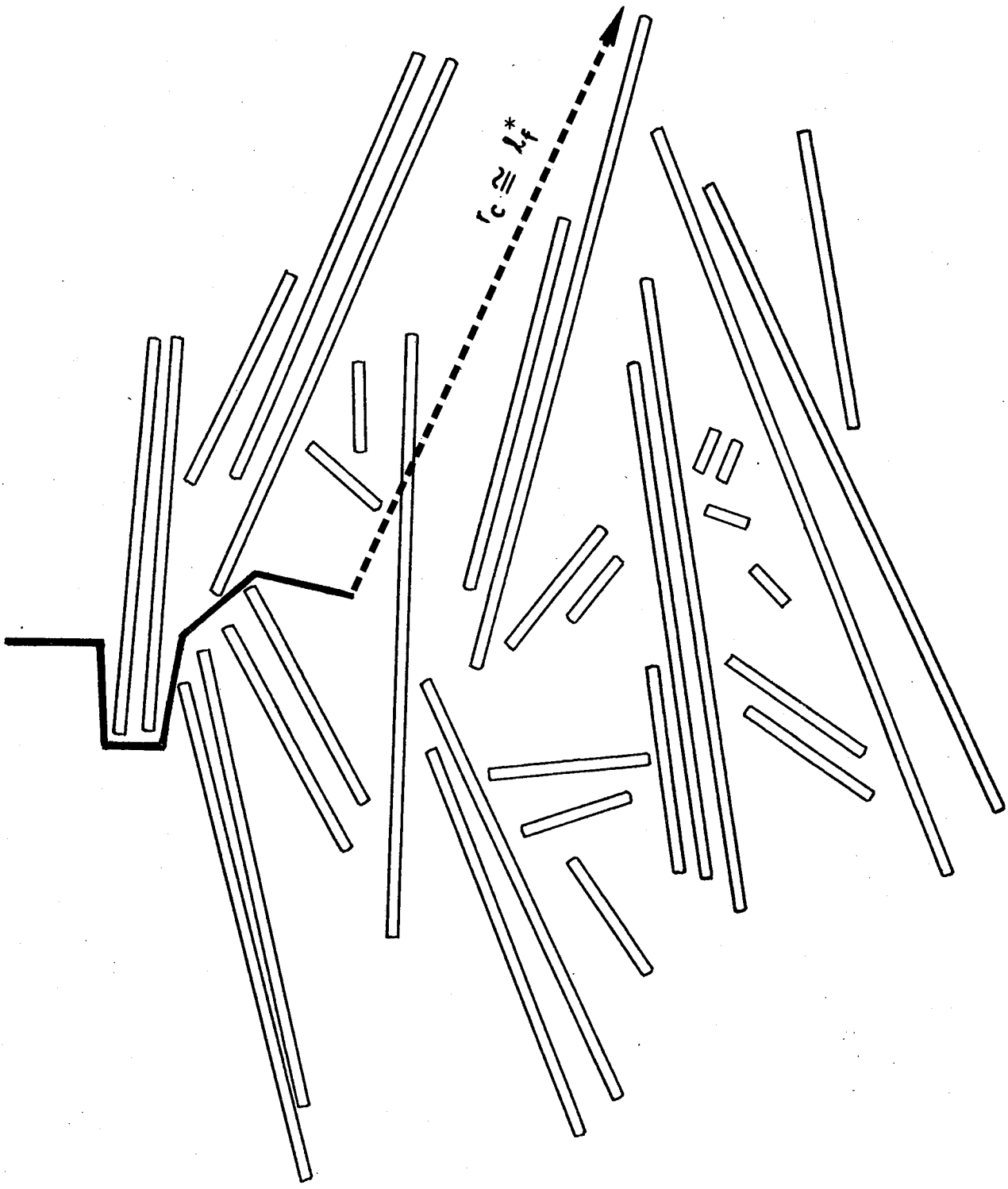

FIGURE 15.

MODEL FOR CRITICAL CRACK TIP ZONE RADIUS FOR FIBER-AVOIDANCE MODE OF FRACTURE.